Modelling Simul. Mater. Sci. Eng. **7** (1999) 383–395. Printed in the UK PII: S0965-0393(99)02926-5

Convergence issues in molecular dynamics simulations of highly entropic materials

Z Zhou and B Joós†

Ottawa Carleton Institute of Physics, University of Ottawa Campus, Ottawa, Ontario, Canada, K1N-6N5

E-mail: zhouz@physics.uottawa.ca

E-mail: joos@physics.uottawa.ca

Received 14 December 1998, accepted for publication 17 March 1999

Abstract. When studying the structural properties of highly entropic materials, the usual criteria for the choice of the time step, the stability of the energy and the pressure, are not always appropriate as they may lead to a time step which is an order of magnitude too large. Two different methods, the stress–strain and equilibrium fluctuation methods, are used to calculate the shear modulus and compared to illustrate this point.

1. Introduction

The molecular dynamics (MD) simulation method, which solves the classical equations of motion numerically for a set of particles, has been widely used to probe both the microscopic and the macroscopic properties of materials.

One of the most important issues in MD is the rate of convergence. The equations of motion are solved by a discretized integration. The choice of the integration step, or time step δt must be small compared to the time scale of microscopic changes in the system. On the other hand, the simulation time which is finite by essence, must be long enough to sample most of the phase space. As a consequence, choosing a time step that is too small is inefficient since it leads to very long computational times. To choose the most efficient time step and time duration in a simulation, the most common approach is to monitor the variations with time of some of the more easily obtained macroscopic quantities, such as the energy, pressure and lattice parameters. Fortunately, in many systems such as crystals, gases and simple liquids, these quantities, as well as other physical quantities of interest, settle down very fast, so the optimum time step and time duration can be determined without difficulty. However, whether such an approach is also appropriate for inhomogeneous soft systems, especially those that do not have a well defined ground state configuration, is not clear.

We present in detail one example where the usual procedures lead to a time step that is an order of magnitude too large to faithfully follow the fluctuations in the system. The system in question is a crosslinked polymer melt (CPM). Its shear modulus was calculated using two different methods. In the first method the shear modulus is obtained from the changes in the stress (or pressure) tensor. We call this a macroscopic measurement and label it μ_{ss}. In contrast, in the second method, the shear modulus is extracted from the microscopic fluctuations in the

† To whom correspondence should be addressed.

0965-0393/99/030383+13$19.50

system. We label this second measurement $\mu_{\rm ef}$. The effect of the choice of the time step on the simulation of the system's properties will be investigated by comparing the agreement between the two methods.

Requiring that the results from both methods converge to the same values is suggested as a means of selecting the optimum time step.

We also see in these systems a noticeably different convergence rate for quantities of different order of the derivative of the free energy.

Similar results are found for another system, a diluted two-dimensional (2D) central force network.

2. Calculation of the shear modulus

Here, we present a brief description of the two methods used to obtain the elastic constant for pure shear deformation. This is a volume preserving deformation, where the system is elongated in one direction, and appropriately compressed in the other two directions. The type of deformation observed when rubber is elongated. The first method is the stress-strain method (SSM). The modulus for pure shear is obtained from the changes in the applied stress tensor $S_{\alpha\beta}$ (negative for compression) under a strain represented by the Lagrangian strain tensor η [1]

$$\mu_{\rm ss} \equiv \frac{(S_{11}(\eta) - S_{11}(0)) - (1/3){\rm tr}(\boldsymbol{S}(\eta) - \boldsymbol{S}(0))}{2\eta_{11}}. \tag{1}$$

Note that equation (1) requires $S_{\alpha\beta}(0)$ which may be anisotropic. What is actually calculated is

$$\mu_{\rm ss} \equiv \frac{S_{11}(\eta) - (1/3){\rm tr}\boldsymbol{S}(\eta)}{2\eta_{11}} \tag{2}$$

which assumes that $S_{\alpha\beta}(0) = 0$. The off-diagonal elements of $S_{\alpha\beta}(0)$ are small and of no concern. There are, however, due to finite size effects non-negligible diagonal elements $S_{\alpha\alpha}(0)$. The simplest way to eliminate these frozen-in stresses in the undeformed sample is to perform the deformation of every sample in the three Cartesian directions in turn, for each crosslinking [1], as we did in this work. The deformation of a sample in one Cartesian direction is, therefore, called a realization and every sample yields three realizations.

The second method is the equilibrium fluctuation method (EFM) which calculates directly the elastic constants from the microscopic fluctuations of the system over time without the need to impose deformations. All elastic constants are obtained from a single run. We have chosen the deformation carefully so that the systems remain in the linear stress-strain regime where the elastic constants are constant. Therefore, the deformed and undeformed states should yield the same results. By doing so computational time is greatly reduced since we can calculate both $\mu_{\rm ef}$ and $\mu_{\rm ss}$ simultaneously in the deformed state. This was done for most samples in this work. In the EFM method, the modulus $\mu_{\rm ef}$ for pure shear for a three-dimensional (3D) system is given by [1]

$$\mu_{\rm ef} = \tfrac{1}{6}[2c_{11} - c_{12} - c_{13} - c_{21} - c_{31} + \tfrac{1}{2}(c_{22} + c_{23} + c_{32} + c_{33})] \tag{3}$$

where the $c_{\alpha\beta}$ are the elastic stiffness coefficients [2, 3] in the condensed Voigt notation. The elastic stiffness coefficients are defined by

$$S_{\alpha\beta}(\eta) = S_{\alpha\beta}(0) + c_{\alpha\beta\sigma\tau}\eta_{\sigma\tau} \tag{4}$$

for a system without internal torques [2–4].

Correspondingly, for a 2D system under an area preserving deformation, the shear modulus can be found from

$$\mu_{\rm ss} \equiv \frac{S_{11} - S_{22}}{4\eta_{11}} \tag{5}$$

and/or

$$\mu_{\mathrm{ef}} = \frac{c_{11} + c_{22} - c_{12} - c_{21}}{4}. \tag{6}$$

For a central force system the isothermal elastic stiffness coefficients can be calculated from [2]

$$\begin{aligned} c_{\alpha\beta\sigma\tau} = {} & \frac{1}{V}\left\langle \sum_{i<j} \Delta x_\alpha(ij)\Delta x_\beta(ij)\Delta x_\sigma(ij)\Delta x_\tau(ij)\frac{1}{r^2}\left(\Phi'' - \frac{\Phi'}{r}\right)\right\rangle \\ & -\frac{1}{k_{\mathrm{B}}TV}\left\langle \delta\left(\sum_{i<j}\Delta x_\alpha(ij)\Delta x_\beta(ij)\frac{\Phi'}{r}\right)\delta\left(\sum_{i<j}\Delta x_\sigma(ij)\Delta x_\tau(ij)\frac{\Phi'}{r}\right)\right\rangle \\ & -\frac{1}{2V}\left(2\left\langle \sum_{i<j}\Delta x_\alpha(ij)\Delta x_\beta(ij)\frac{\Phi'}{r}\right\rangle\delta_{\sigma\tau} - \left\langle \sum_{i<j}\Delta x_\alpha(ij)\Delta x_\sigma(ij)\frac{\Phi'}{r}\right\rangle\delta_{\beta\tau}\right. \\ & -\left\langle \sum_{i<j}\Delta x_\alpha(ij)\Delta x_\tau(ij)\frac{\Phi'}{r}\right\rangle\delta_{\beta\sigma} - \left\langle \sum_{i<j}\Delta x_\beta(ij)\Delta x_\tau(ij)\frac{\Phi'}{r}\right\rangle\delta_{\alpha\sigma} \\ & \left.-\left\langle \sum_{i<j}\Delta x_\beta(ij)\Delta x_\sigma(ij)\frac{\Phi'}{r}\right\rangle\delta_{\alpha\tau}\right) + \frac{Nk_{\mathrm{B}}T}{V}\delta_{\alpha\beta}\delta_{\sigma\tau}. \end{aligned} \tag{7}$$

The stress tensor is given by

$$S_{\alpha\beta} = \frac{1}{V}\left\langle \sum_{i<j}\Delta x_\alpha(ij)\Delta x_\beta(ij)\frac{\Phi'}{r}\right\rangle - \frac{Nk_{\mathrm{B}}T}{V}\delta_{\alpha\beta} \tag{8}$$

where $\langle \ldots \rangle$ indicate configurational averages and $\delta(A) = A - \langle A \rangle$, $\Delta x_\alpha(ij)$ and r are defined as

$$\Delta x_\alpha(ij) = x_\alpha(i) - x_\alpha(j) \tag{9}$$

$$r^2 = \mid \Delta x_\alpha(ij) \mid^2 . \tag{10}$$

x represents the coordinates of N particles, Φ the interparticle interaction potential and V the volume of the system. The first term (positive) in equation (7) is referred to as the 'Born term'. In the absence of stress, and at zero temperature, it is the only term in a homogeneous system. The second term (negative) is the 'fluctuation term'. The third term is the 'stress term' and the last is sometimes called the 'kinetic term' [5]. We should emphasize that the volume V which appears in equations (7) and (8) must be the current (stressed) one [2], instead of the volume of the stress-free state. The dominant terms are the first two: the Born term is positive while the fluctuation term is negative.

The EFM provides a way to obtain all elastic constants from a single run and has the advantage that no actual deformations are made, so no symmetry breaking occurs. It should be very accurate since the elastic constants are obtained from averages over all microscopic fluctuations in the system, in contrast with the SSM which averages over the macroscopic fluctuations of the finite sample. The EFM has been successfully applied to crystalline materials where there is a well defined ground-state configuration in the system. However, for materials which are intrinsically inhomogeneous with a large number of configurations close in energy, such as glasses, metallic or polymeric and the CPM, it is not at all clear how well such a method will work.

3. The systems studied

3.1. The crosslinked polymer melt

We focus on the crosslinked polymer melt (CPM), the simplest model for rubber, because it has not only a large number of possible configurations of equal or very similar energy, but it is also a good example of a special class of materials which derive their elasticity not from potential energy changes, but from changes in the entropy. In a process known as vulcanization [6], crosslinks between molecules on different polymers in the melt convert the system from a fluid to an amorphous solid with non-zero shear modulus. This solid phase is of interest because of its remarkable elastic properties which are of technological and biological relevance. The onset of rigidity is itself an interesting problem because of its connection to percolation and the predictions that have been made by de Gennes on the variation of the shear modulus with crosslink density [7]. The vulcanization transition has also received some recent attention with the development of a replica theory by Goldbart and co-workers [8]. A recent review of these topics can be found in [9].

In a recent collaborative work, in which we were involved [1], the shear modulus of CPMs was calculated using the SSM. These were very time-consuming calculations. Averages were made to converge using many realizations, which in spite of lengthy simulation times did not individually converge. In the same paper [1], it was also reported that the EFM [2] failed to measure a finite shear modulus even after a million time steps, when the SSM showed a rigid solid. This discrepancy could not be explained since both methods ought to give the same answer. In this paper we will clarify this problem.

Our model of polymers is the same as that used in an extensive set of calculations by Kremer and Grest [10]. In their model, all particles in the system interact through a purely repulsive truncated Lennard-Jones potential

$$\Phi_{\mathrm{LJ}}(r_{ij}) = \begin{cases} 4\epsilon\left[\left(\dfrac{\sigma}{r_{ij}}\right)^{12} - \left(\dfrac{\sigma}{r_{ij}}\right)^{6} + \dfrac{1}{4}\right] & r_{ij} < 2^{1/6}\sigma \\ 0 & r_{ij} \geqslant 2^{1/6}\sigma \end{cases} \tag{11}$$

which ensures self-avoidance. On a given chain, there is an added attractive potential [11] between nearest neighbours

$$\Phi_{\mathrm{nn}}(r_{ij}) = \begin{cases} -\dfrac{1}{2}kR_0^2 \ln\left[1 - \left(\dfrac{r_{ij}}{R_0}\right)^2\right] & r_{ij} < R_0 \\ \infty & r_{ij} \geqslant R_0 \end{cases} \tag{12}$$

with $R_0 = 1.5\sigma$ and $k = 30\epsilon/\sigma^2$. The combination of these two potentials prevents polymers from passing through each other.

We denote the number of polymers in the system by M, the number of monomers on each chain by N and the crosslink density, i.e. the number of crosslinks per chain, by n. In this paper, we focus on the case $M = 100$, $N = 10$ and $n = 2$ (the critical density of rigidity $n_{\mathrm{c}} \approx 1.01$ [9, 12]). With this choice of polymer length, there will be few entanglements since the entanglement length of our system is of the order of 35 monomers [10]. Entropic effects come from collisions and constraints in the vibrational amplitudes of the chains. The density of the system is $\rho\sigma^3 = 0.85$. The simulations were done at a temperature $k_{\mathrm{B}}T/\epsilon = 4.0$ with a constant temperature molecular dynamics code using a standard damped force velocity Verlet algorithm [13, 14] and periodic boundary conditions.

The polymer melt was first equilibrated without crosslinks. The crosslinks were then randomly placed as reported in [1]. Crosslinking between nearest neighbours on the same

chain was not permitted nor was there more than one link between any pair of particles allowed. To avoid having the system trapped in metastable states, we submitted it to a heating-quenching process. The unit of time was $t_0 = \sqrt{m\sigma^2/\epsilon}$ and three values of the time step $\delta t_1 = 0.005t_0$, $\delta t_2 = 0.0025t_0$ and $\delta t_3 = 0.00125t_0$ were used in the work. When using the last two time steps, we first heated the system up to $k_BT/\epsilon = 8.0$, equilibrated it for 25 000 time steps and then annealed it down to $k_BT/\epsilon = 4.0$ in 50 000 time steps. Most of the samples were again equilibrated for 50 000 time steps before calculating the quantities of interest. We also equilibrated several samples up to 200 000 time steps but found no significant effect on the results. Barsky *et al* reported a relaxation time of $0.05t_0$ for the pressure tensor obtained from its autocorrelation functions (see figure 2 in [1]). The relaxation time for μ_{ss} measured from the starting initial configuration is, however, of the order of $5t_0$ as shown in figure 3 of [1]. This is in accordance with what will be shown in section 4.1. $5t_0$ corresponds to 2000 and 4000 time steps for δt_2 and δt_3, respectively. Barsky and Plischke have also shown that there is no evidence of ergodicity breaking or sectioning of phase space in this system [15].

The deformation of the MD cell is done at a strain rate of $10^{-4}(\lambda_\alpha - 1)L_\alpha/\delta t_i$, from $L_\alpha \rightarrow \lambda_\alpha L_\alpha$, where L_α with $\alpha = 1, 2$ and 3 are the lengths of the cell along the three Cartesian coordinate axes. We chose $\lambda_1 = \lambda, \lambda_2 = \lambda_3 = 1/\sqrt{\lambda}$ so that $\lambda_1\lambda_2\lambda_3 \equiv 1$, i.e. we applied a pure shear or volume preserving deformation ($\eta_{11} = \lambda - 1$). We took $\lambda = 1.1$ for most realizations. The deformation has to be large enough that the change in the stress tensor can be well resolved, but small enough to remain within the linear stress-strain regime (equation (4)). We found that μ increases rapidly only for $\lambda > 1.5$, which gives us a large workable interval of deformation.

3.2. The two-dimensional diluted central force network

The other system discussed is a 2D diluted central force network (DCFN), which has been used to show that the onset of mechanical rigidity occurs at a concentration of bonds and sites which is significantly larger than the percolation threshold [16]. It is simply a triangular network of springs of equal equilibrium length r_0 which is diluted by removing sites randomly. In this system, the nearest neighbours interact via the circularly symmetric potential $V_{nn}(r_{ij}) = \frac{1}{2}k(r_{ij} - r_0)^2$ and more distant neighbours are non-interacting. For this system, geometric percolation occurs at a concentration of bonds $p_c = 0.5$ and rigidity percolation (at $T = 0$) at $p_r \approx 0.71$. The regime of interest for this study is the interval $p_c < p < p_r$ where, at zero temperature, the system is not rigid, but at finite temperature develops a finite shear modulus of entropic origin [17]. λ was chosen to be 1.001. The reason for choosing such a small deformation is that we found that at very low T, $\lambda = 1.05$ leads to a considerable (about 10%) discrepancy of both μ_{ss} and μ_{ss} from the exact result for the perfect lattice, $(\sqrt{3}/4)k$, at zero T [18]. The unit of time is $t_0' = \sqrt{k/m}$ and the unit of temperature is kr_0^2/k_B. The size of the system used to discuss the effect of time steps and time duration is 16×16 sites.

4. The impacts of the time step and the time duration

4.1. The crosslinked polymer melt

For the crosslinked polymer melt, it was found that in the constant energy ensemble [1, 15] using $\delta t_1 = 0.005t_0$ the energy can be stabilized to 1 part in 10^4 and the average pressure tensor to 1 part in 10^3 over the length $6 \times 10^5\delta t_1$ of a run. Therefore, δt_1 was used to calculate μ_{ss} and the order parameters [15] for various system sizes. Good convergence results were obtained [1, 15]. This time step also gives a reasonable behaviour for μ_{ss} and μ_{ef} at very high

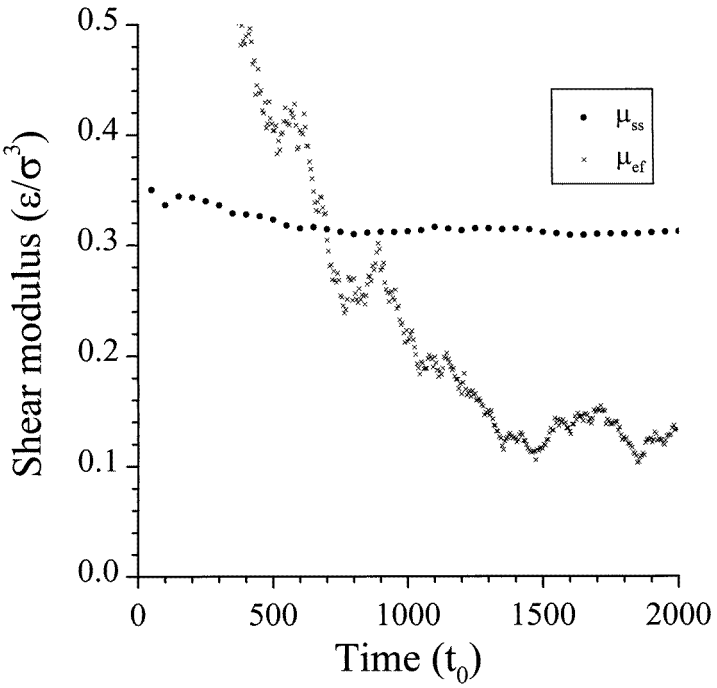

Figure 1. The average of μ_{ss} and μ_{ef} of 63 realizations up to $8 \times 10^5 \delta t_1$ against time for CPM with $N = 10$, $M = 100$ and $n = 2$.

crosslink density n. For instance, in a system with $M = 30$, $N = 20$ and $n = 12$, we found that $\mu_{ef}/\mu_{ss} = 0.974$ from an average over 10 samples, as was reported in an earlier paper [1]. However, in that paper [1] we also reported that at a moderate n, μ_{ef} shows a very poor behaviour and seems to always tend to zero. This is obviously inconsistent with μ_{ss}. It raises the question as to whether the EFM works properly for this kind of material. Note that the problem is essentially caused by the 'fluctuation term' in the EFM which is the more sensitive. So an accurate calculation of the fluctuations in the system is important.

There are several possible factors that may contribute to the disagreement. For instance, a deformation of the cell that is too large will lead to a departure from the linear range of the stress-strain relation so that μ_{ss}, the average shear modulus, will not necessarily be equal to μ_{ef}, the shear modulus of the deformed state. This source of error can be ruled out because, as mentioned before, we have a large interval of workable deformations. Finite size effects may be a possible source of disagreement, because they manifest themselves differently in the two methods; the SSM is self-averaging whereas the EFM is not. More serious sources of error are the size of the time step and the length of the run.

First, we found that, with time step δt_1, μ_{ss} for most individual realizations did not converge to a well defined limit up to the completion time. It was, therefore, natural to reduce the time step to stabilize it. We reduced it first from $\delta t_1 = 0.005 t_0$ to $\delta t_2 = 0.0025 t_0$. This improved the stability of the average energy and pressure tensor to 1 part in 10^5 and 1 part in 10^4, respectively. We then performed simulations with $n = 2$ on 21 deformed samples (63 realizations) up to $8 \times 10^5 \delta t_2$.

After averaging over all 63 deformed realizations, we obtained the results shown in figure 1. The average μ_{ss} has a small variation and converges well to about $0.308\epsilon/\sigma^3$, but μ_{ef} is

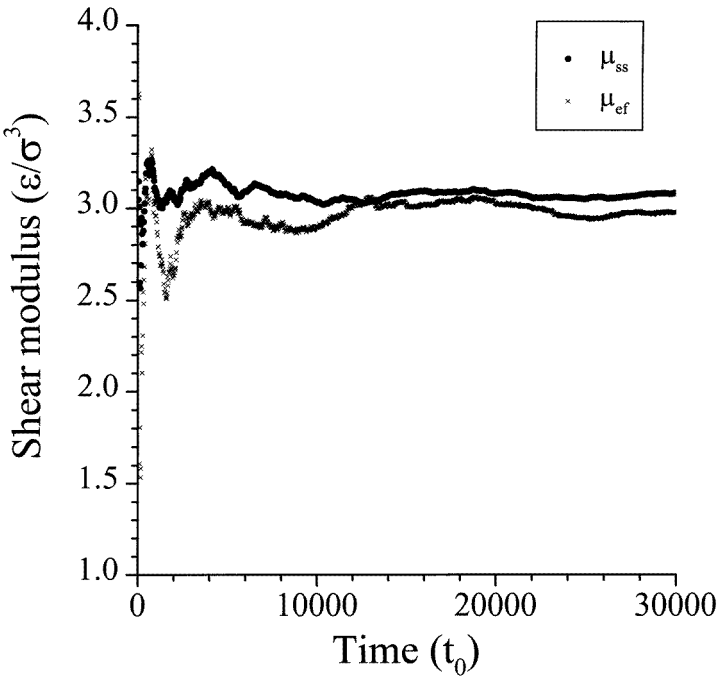

Figure 2. The average of μ_{ss} and μ_{ef} of two samples up to $1.2 \times 10^7 \delta t_2$ against time for CPM with $N = 10$, $M = 100$ and $n = 5$.

obviously smaller than μ_{ss} and its time evolution shows no clear trend. Convergence of the μ_{ss} for individual realizations did improve also by using $\delta t_2 = 0.0025 t_0$, but they still did not converge to a well defined limit at the completion time of the run.

To verify the expressions for the EFM and also whether the magnitude of the deformation is appropriate, we then performed simulations on a rather high crosslink density $n = 5$ for two samples and up to $1.2 \times 10^7 \delta t_2$. At this density the system is quite rigid so that μ_{ef} should agree well with μ_{ss} if the deformation is small. Figure 2 shows the average results for these two samples. The two methods basically agree. More samples would improve the agreement, but it is not necessary to increase the running time.

Returning to $n = 2$, we ran four samples (12 realizations) up to $8 \times 10^6 \delta t_2$, and still found very poor agreement between μ_{ss} and μ_{ef}. These 12 long runs show some common features: (1) after several million δt_2, almost all μ_{ss} (11 of 12 realizations) converge; (2) after several millions δt_2, almost all μ_{ef} (11 of 12 realizations) are below μ_{ss}; (3) up to the end of the run, most μ_{ef} values (10 of 12 realizations) are very close or below zero and show no clear trend. A typical example is shown in figure 3. Finally, averaging over all four samples, we found that μ_{ss} converges to $0.295\epsilon/\sigma^3$ after $6 \times 10^6 \delta t_2$, which agrees well with the values obtained from 21 moderate time samples, $0.308\epsilon/\sigma^3$. However, μ_{ef} shows no clear trend even up to $8 \times 10^6 \delta t_2$, as shown in figure 4, and has an analogous behaviour as that obtained from 21 moderate time runs (figure 1). This applies to every individual realization, as shown in figure 3.

Therefore, summing up to this point, we find that with δt_2, the length of the simulation runs, the number of realizations, and the magnitude of the deformation play no role in the inconsistency between μ_{ss} and μ_{ef}. We then applied the EFM to the undeformed pure melts ($n = 0$) running up to $5 \times 10^6 \delta t_2$. The pure polymer melts must be a fluid with a zero shear modulus. However, μ_{ef} behaved very poorly again, as can be seen in figure 5(a).

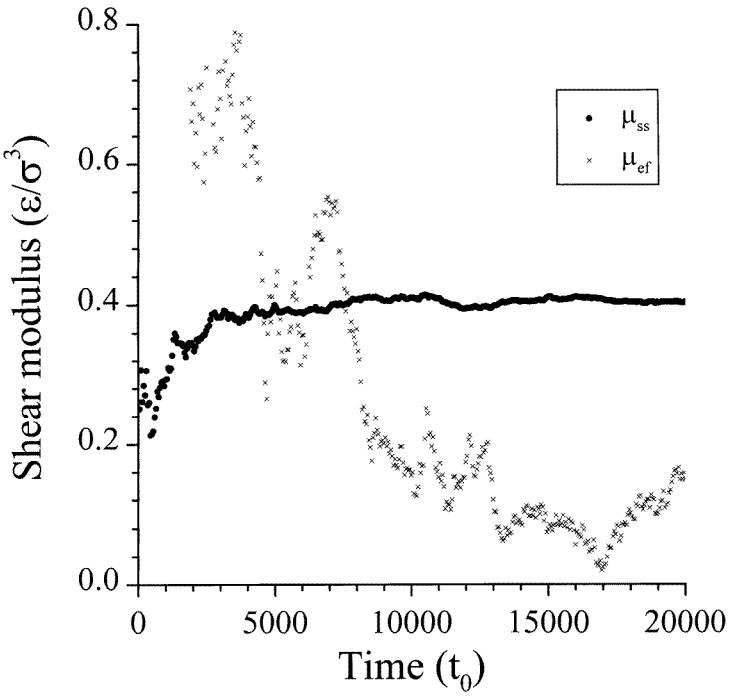

Figure 3. μ_{ss} and μ_{ef} of a typical realization up to $8 \times 10^6 \delta t_2$ against time for CPM with $N = 10$, $M = 100$ and $n = 2$.

It seemed that the time step was still too large to properly follow the fluctuations in the system. There is a configuration fluctuation term in the expression of μ_{ef} (see equation (7)). A time step that is too large may lead to non-physical configuration fluctuations which depress μ_{ef}. Some parts of the system appear to be constantly in unstable states. Therefore, we reduced the time step further from δt_2 to $\delta t_3 = 0.00125 t_0$ and applied the EFM to the undeformed pure melts up to $10^7 \delta t_3$. Figure 5(b) shows the average of μ_{ef} over two realizations. We can see that μ_{ef} goes from being greater than one at the beginning to about zero at about $2 \times 10^6 \delta t_3 = 2500 t_0$ and then oscillates toward zero. Individual realizations show the same behaviour but have a slightly larger oscillation.

The fact that by using δt_3 we got $\mu_{ef} = 0$ for every realization of the pure melt provides strong evidence that the EFM can also work properly for this model system but it requires a very small time step. Long relaxation times are required due to the viscous nature of the material. An analogy is the behaviour of viscoelastic materials which under a periodic stress of frequency higher than some critical value show no deformation. The threshold frequency corresponds to the inverse of the response time of the substance and the material takes a long time to equilibrate. A careful preparation of the system can help matters. For this reason we applied a heating-quenching technique to the system as mentioned in section 2. However, this also suggests that one should be very careful in explaining the results obtained from moderate time runs. For example, if we stopped the simulation after $1.6 \times 10^6 \delta t_3 = 2000 t_0$, we would conclude that the pure melt has a finite $\mu_{ef} \approx 0.35 \epsilon/\sigma^3$ instead of zero.

Finally we ran four deformed samples (12 realizations) with $n = 2$ up to $8 \times 10^6 \delta t_3$. Figure 6 shows the average results over these four samples with $\mu_{ef} \approx \mu_{ss} = 0.280 \epsilon/\sigma^3$. The disagreement between μ_{ss} and μ_{ef} is greatly reduced but μ_{ef} still converges considerably

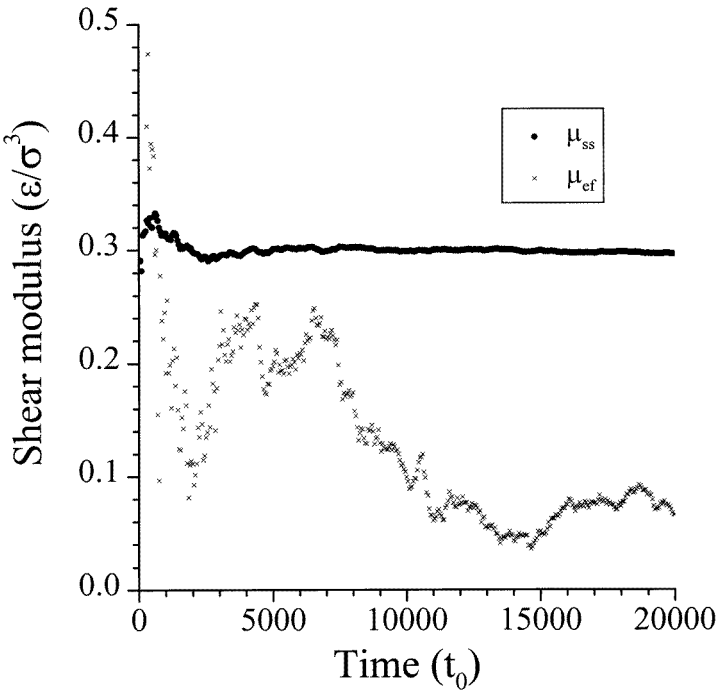

Figure 4. The average of μ_{ss} and μ_{ef} of four samples up to $8 \times 10^6 \delta t_2$ against time for CPM with $N = 10$, $M = 100$ and $n = 2$.

slower than μ_{ss}. We can expect that more samples will improve the agreement further but longer times are of little help. We ran one realization up to $3.2 \times 10^7 \delta t_3$, as shown in figure 7, but this individual μ_{ef} is not yet stable even after such a long time. This is similar to what is observed for $n = 5$ with time step δt_2. It is reasonable to think that a further reduction in the time step would have a larger impact on the convergence of μ_{ef} than increasing the length of the runs with the current time step. The reduction in time step seems to also have an effect on μ_{ss} which decreases somewhat with decreasing time steps (from $0.308\epsilon/\sigma^3$ to $0.280\epsilon/\sigma^3$), but more runs would be required to confirm this.

There is a clear correspondence in this system between the convergence rate of a quantity and the order of the derivative of the free energy upon which it depends. We found that for an *individual* realization, the energy settles down to 1 part in 10^5 within $10^4 \delta t_3$, the pressure tensor to 1 part in 10^4 within $5 \times 10^4 \delta t_3$. In contrast, μ_{ss} settles down to 5 parts in 10^2 within $2 \times 10^6 \delta t_3$, as shown in figure 7, but μ_{ef} has still not converged at $10^7 \delta t_3$. The pressure is the first derivative of the free energy, μ_{ef} corresponds to the second derivative of the free energy and μ_{ss} is somewhere between the first and the second derivative of the free energy. μ_{ss} is obtained from a finite deformation and, therefore, is an average rate of stress response with respect to strain from the initial to the final state.

4.2. The two-dimensional diluted central force network

For the DCFN described in section 3.2, similar results are found. In studies of melting of the perfect lattice, with a cut-off harmonic potential known as the piecewise-linear restoring force potential, Combs [19] used a time step $0.1t_0'$. In work on vacancy annealing kinetics [20, 21],

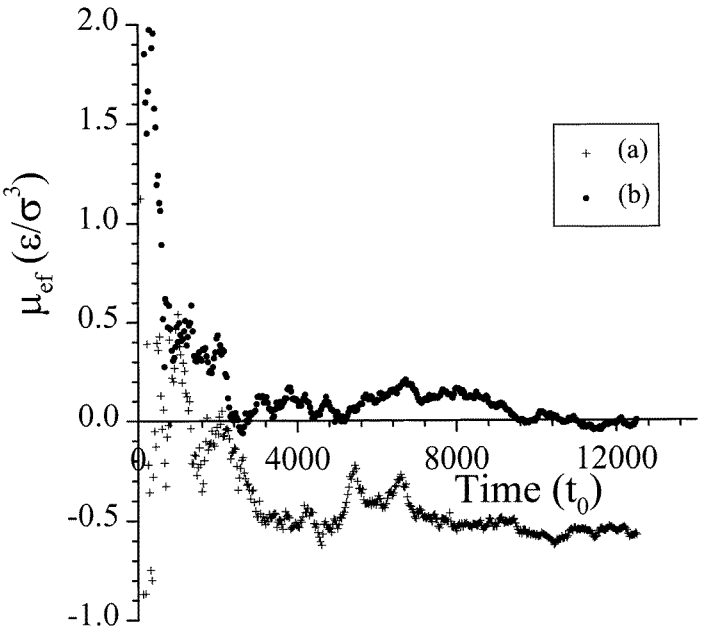

Figure 5. (a) The variation of μ_{ef} up to $5 \times 10^6 \delta t_2$ against time for pure polymer melts, $N = 10$, $M = 100$ and $n = 0$; (b) the variation of average μ_{ef} over two realizations up to $10^7 \delta t_3$ against time for pure melt.

and membrane rupture [18] on the same system, we used, respectively, 0.1 and $0.05t_0'$. The behaviour of these systems in all respects was perfectly reasonable. In the DCFN at high density, $\delta t = 0.05t_0'$ still works well. For instance, at density $p = 0.85$ and $T = 0.005kr_0^2/k_B$, the agreement between μ_{ss} and μ_{ef} from 30 samples up to $10^6\delta t$ is almost perfect, and is very similar to the result of CPM at high crosslinking density. However, at low density where the entropy is significant, $\delta t = 0.05t_0'$ was clearly too large, yielding at the same temperature as before depressed μ_{ss} values, sometimes even negative values, and enhanced μ_{ef} values, the reverse of that observed in the CPM. For instance, at the density $p = 0.6$, using $\delta t = 0.05t_0'$ we found that $\mu_{ef} > 0.05$ but $\mu_{ss} < -0.06$. With $\delta t = 0.005t_0'$ up to 10^6 time steps and an average over 150 samples, the agreement between the two calculations is still very poor, and μ_{ss} and μ_{ef} even have different trends, as shown in figure 8(a). The same poor agreement and different trends between μ_{ss} and μ_{ef} were observed for this system with $\delta t = 0.01t_0'$ up to 10^6 time steps and an average over 100 samples. In this system the ground-state configuration for a given sample is well defined, and so not the source of the error. Good agreement was obtained when $\delta t = 0.0016t_0'$ was used, as shown in figure 8(b), and after an extrapolation using $\mu_{ef}(t) = \mu_{ef}(\infty) + (a/t)$, $\mu_{ss}(t) = \mu_{ss}(\infty) + (a'/t)$, we found $\mu_{ef} = \mu_{ef}(\infty) = 0.00865k$ and $\mu_{ss} = 0.00878k$. Agreement between μ_{ef} and μ_{ss} improves with increasing numbers of samples. In a recent letter on rigidity near the threshold $\delta t = 0.0016t_0'$ was used [17].

These results add weight to our findings on the crosslinked polymer melt showing that the difficulties encountered there are not unique. In the DCFN we found that μ_{ef} goes down but μ_{ss} goes up when the time step is reduced, the opposite behaviour to that observed in the CPM. At $\delta t = 0.01t_0'$ up to 10^6 time steps and an average over 100 samples, either μ_{ef} or μ_{ss} does not converge well but we see that $\mu_{ef} > 0.01k$ and $\mu_{ss} < 0.0075k$. At $\delta t = 0.005t_0'$ up to 10^6

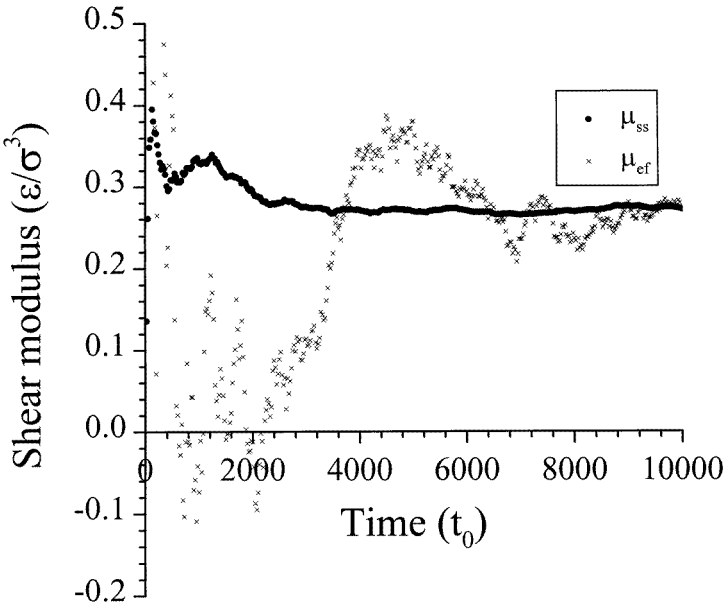

Figure 6. The average of μ_{ss} and μ_{ef} of 12 realizations up to $8 \times 10^6 \delta t_3$ against time for CPM with $N = 10$, $M = 100$ and $n = 2$.

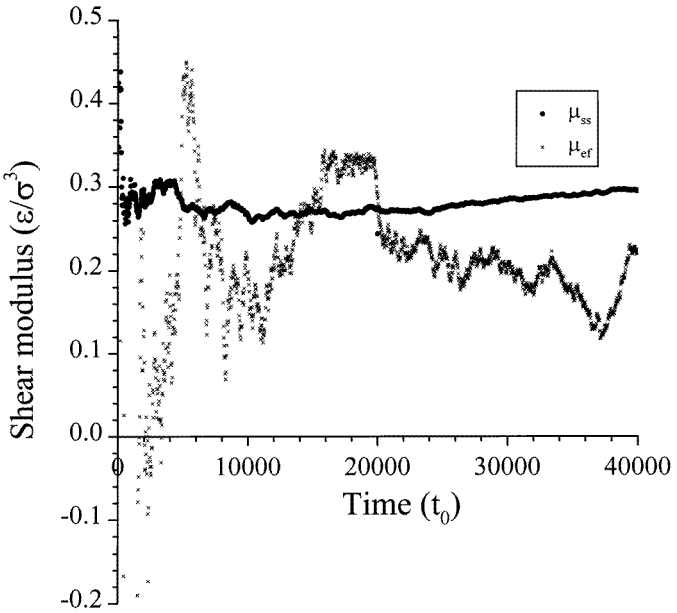

Figure 7. μ_{ss} and μ_{ef} of a typical realization up to $3.2 \times 10^7 \delta t_3$ against time for CPM with $N = 10$, $M = 100$ and $n = 2$.

time steps and an average over 150 samples, μ_{ss} does not converge well and $\mu_{ss} < 0.0075k$ as shown in figure 8(a). However, μ_{ef} converges to the extrapolated value $\approx 0.010k$; this is a significantly larger value than that found with $\delta t = 0.0016t_0'$.

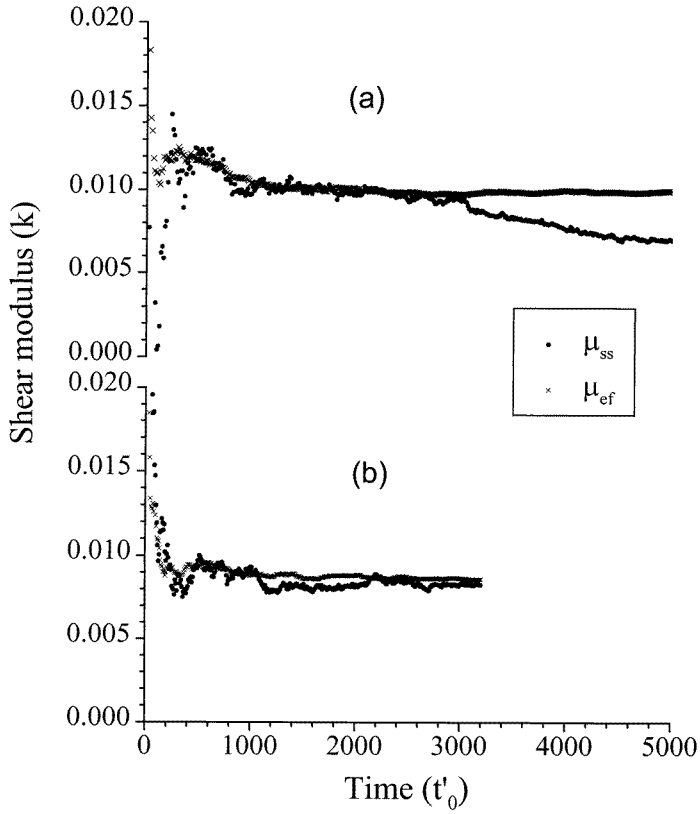

Figure 8. (a) The average of μ_{ss} and μ_{ef} of 150 samples up to 10^6 time steps against time for site-diluted triangular networks at $p = 0.6$. The time step is $0.005t_0'$. (b) The average of μ_{ss} and μ_{ef} of 260 samples up to 2×10^6 time steps against time for site-diluted triangular networks at $p = 0.6$. The time step is $0.0016t_0'$.

5. Conclusions

As expected, the two methods used to calculate the elastic constants can be made to agree by decreasing the time step. The EFM method measuring fluctuations is, in particular, sensitive to the time step for the system without a well defined ground-state configuration, the crosslinked polymer melt (CPM). The minimum acceptable time step in this kind of system is smaller than for the stress-strain method. This is clearly illustrated by our results.

Whichever method is more efficient and stable depends on the system studied. However, good convergence should not be mistaken with accuracy, in particular, when individual realizations do not converge. The agreement of the two methods and properly simulated fluctuations increase confidence in the final results.

We conclude by stating that the usual criteria for the choice of the time step, i.e. the stability of the energy and the pressure are not always sufficient to ensure a faithful simulation of the properties of a system, especially if fluctuations are large, as is the case in crosslinked polymer networks (CPM) close to the onset of rigidity. When studying quantities which are a function of the fluctuations or dynamical properties, the proper time step may be one order of magnitude smaller than the one usually chosen. Requiring agreement between a macroscopic

measurement μ_{ss} and a microscopic average, obtained through a fluctuation-dissipation type formula μ_{ef} can become a new convergence criteria for structural properties.

Note added in proof. We looked for ergodicity breaking in DCFN using the method described in [22, 23] but did not find any. The critical time steps are sensitive to the method used to maintain the temperature at a constant.

Acknowledgments

This work has been supported by the Natural Sciences and Engineering Research Council of Canada. Stimulating discussions with Michael Plischke are gratefully acknowledged.

References

[1] Barsky S J, Plischke M, Joós B and Zhou Z 1996 *Phys. Rev.* E **54** 5370
[2] Zhou Z and Joós B 1996 *Phys. Rev.* B **54** 3841
[3] Wang J, Yip S, Phillpot S R and Wolf D 1993 *Phys. Rev. Lett.* **71** 4182
Wang J, Li J, Yip S, Phillpot S and Wolf D 1995 *Phys. Rev.* B **52** 12 627
[4] Barron T H K and Klein M L 1965 *Proc. Phys. Soc.* **85** 523
[5] Squire D R, Holt A C and Hoover W G 1969 *Physica* **42** 388
[6] Treloar L R G 1975 *The Physics of Rubber Elasticity* (Oxford: Clarendon)
Treloar L R G 1973 *Rep. Prog. Phys.* **36** 755
[7] de Gennes P G 1976 *J. Physique Lett.* **37** L1
de Gennes P G 1977 *J. Physique Lett.* **38** L355
[8] Goldbart P M, Castillo H E and Zippelius A 1996 *Adv. Phys.* **45** 393
Castillo H E and Goldbart P M 1998 *Phys. Rev.* E **58** R24
[9] Plischke M and Joós B 1997 *Phys. Canada* **53** 184
[10] Kremer K and Grest G S 1990 *J. Chem. Phys.* **92** 5057
[11] Bird R B, Armstrong R C and Hassager O 1977 *Dynamics of Polymeric Liquids* vol 1 (New York: Wiley)
[12] Plischke M and Barsky S 1998 *Phys. Rev.* E **58** 3347
[13] Brown D and Clarke J H R 1984 *Mol. Phys.* **51** 1243
[14] Allen M P and Tildesley D J 1987 *Computer Simulation of Liquids* (New York: Oxford University Press)
[15] Barsky S J and Plischke M 1996 *Phys. Rev.* E **53** 871
[16] Feng S and Sen P N 1984 *Phys. Rev. Lett.* **52** 1891
Feng S, Thorpe M F and Garboczi E 1985 *Phys. Rev.* B **31** 276
Moukarzel C and Duxbury P M 1995 *Phys. Rev. Lett.* **75** 4055
Jacobs D J and Thorpe M F 1996 *Phys. Rev.* E **53** 3682
[17] Plischke M and Joós B 1998 *Phys. Rev. Lett.* **80** 4907
[18] Zhou Z and Joós B 1997 *Phys. Rev.* B **56** 2997
[19] Combs J A 1988 *Phys. Rev. Lett.* **61** 714
Combs J A 1988 *Phys. Rev.* B **38** 6751
[20] Joós B, Zhou Z and Duesbery M S 1994 *Phys. Rev.* B **50** 8763
[21] Zhou Z and Joós B 1995 *Surf. Sci.* **323** 311
[22] Holian B L, Voter A F and Ravelo R 1995 *Phys. Rev.* E **52** 2338
[23] Simonazzi R and Tenenbaum A 1996 *Phys. Rev.* E **54** 964